



COMMUNICATIONS IN PHYSICS

ISSN 0868 - 3166

Published by
VIETNAM ACADEMY OF SCIENCE AND TECHNOLOGY

Volume 25, Number 2

June 2015

Contents

	Page
Hoang Ngoc Long – Challenges in Particle Physics and 3-3-1 Models	97
Truong Trong Thuc, Le Tho Hue, Dinh Phan Khoi, and Nguyen Thanh Phong – One Loop Corrections to Decay $\tau \rightarrow \mu\gamma$ in Economical 3-3-1 Model	113
Nguyen Quoc Khanh and Mai Thanh Huyen – Transport Properties of a Quasi-two-dimensional Electron Gas in InP/In _{1-x} Ga _x As/InP Quantum Wells: Correlation and Magnetic Field Effects	125
Vuong Son, Nguyen Duc Chien, Truong Thanh Toan, Doan Tuan Anh, Mai Anh Tuan, Luong Thi Thu Thuy, Pham Thi Kim Thanh – Development of Spray Pyrolysis System for Deposition of Nano-structure Materials	133
Tran Thi Thao, Vu Thi Hai, Nguyen Nang Dinh, and Le Dinh Trong – Optical Property and Photoelectrical Performance of a Low-bandgap Conducting Polymer Incorporated with Quantum Dots Used for Organic Solar Cells	139
Bui Trung Ninh, Nguyen Quoc Tuan, Ta Viet Hung, Nguyen The Anh, and Pham Van Hoi – Influence of ASE Noise on Performance of DWDM Networks Using Low-power Pumped Raman Amplifiers	147
Ho Quang Quy, Nguyen Van Thinh, and Chu Van Lanh – Ultrasonic-controlled Micro-lens Arrays in Germanium for Optical Tweezers to Sieve the Micro-particles	157
Nguyen Tuan Khai, Le Dinh Cuong, Do Xuan Anh, Duong Duc Thang, Trinh Van Giap, Nguyen Thi Thu Ha, Vuong Thu Bac, and Nguyen Hao Quang – Assessment of Radioactive Gaseous Effluent Released from Nuclear Power Plant Ninh Thuan 1 under Scenario of Ines-level 5 Nuclear Accident	165
Nguyen Hoang Phuong Uyen, Gajovic-Eichelmann Nenad, Frank. F. Bier, and Ngo Vo Ke Thanh – Investigation of Immobilizing Antigens on Gold Surface by Potentiometric Measurements and Fluorescence Microscopic	173
Vo Thi Lan Anh, Ngo Tuan Ngoc, Doan Minh Chung, K. G. Kostov, and B. I. Vichev – Development of the C-band Radiometer and Its Utilization for Sea Surface Temperature Research in Vietnam	183
ERRATUM: Simulation for Neutron Transport in PWR Reactor Moderator and Evaluation for Proper Thickness of Light Water Reflector – [Nguyen Tuan Khai and Phan Quoc Vuong, <i>Comm. Phys.</i> 25(1) (2015) 91–96]	193

INFLUENCE OF ASE NOISE ON PERFORMANCE OF DWDM NETWORKS USING LOW-POWER PUMPED RAMAN AMPLIFIERS

BUI TRUNG NINH AND NGUYEN QUOC TUAN

VNU University of Engineering and Technology (VNU-UET), Vietnam National University, Hanoi

TA VIET HUNG

Center of High Tech Communications, Department of Telecom, MOD, Vietnam

NGUYEN THE ANH AND PHAM VAN HOI

Institute of Materials Science, VAST, 18 Hoang Quoc Viet Str., Cau Giay Dist., Hanoi, Vietnam

E-mail: ninhbt@vnu.edu.vn

Received 14 March 2015

Accepted for publication 24 June 2015

Abstract. *We present the results of investigation for influence of amplified spontaneous emission (ASE) noise, noise figure (NF) and chromatic dispersion on the performance of middle-distance Dense-wavelength-division-multiplexing (DWDM) networks using low-power pumped distributed Raman amplifiers (DRAs) in two different pump configurations, i.e., forward and backward pumping. We found that the pumping configurations, ASE noise, and dispersion play an important role for improving network performance by decrease of noise figure and bit error rate (BER) of the system. Simulation results show that the lowest bit error rate and low noise figure were obtained, when using forward pumping configuration. Moreover, we have also compared ASE noise powers of the simulation with these of the experiment. These results conclude that DRA with low pump power (< 1 W) is the promising key technology for short- and/or middle-distance DWDM transmission networks.*

Keywords: dense-wavelength-division-multiplexing (DWDM), distributed raman amplifier (DRA), amplified spontaneous emission (ASE).

I. INTRODUCTION

Optical nonlinear effects within optical fiber such as stimulated Raman scattering, stimulated Brillouin scattering or stimulated four-photon mixing may be employed to provide optical amplification by injecting a high-power laser beam into optical fiber. Among these, Raman amplification exhibits advantages of self-phase matching between the pump and signal together with a broad gain-bandwidth in comparison with the other nonlinear processes. Thus it is attractive for current dense wavelength division multiplexed (DWDM) systems since it provides gain over the entire fiber band [1]. One of the most usable in the contemporary submarine and long-haul terrestrial networks is the distributed Raman amplifiers (DRAs) used stimulated Raman scattering (SRS) effect, which has many advantages: stimulated Raman amplification can occur in any fiber at any signal wavelength by proper choice of the pump wavelength; the Raman gain process is

very fast and the effective noise figure (NF) of DRA is smaller than the one of Erbium-doped fiber amplifier (EDFA) and/or the semiconductor optical amplifier [2, 3]. In a DWDM system to reach a long transmission distance and have flat gain-bandwidth a hybrid Erbium-doped fiber (EDFA) and DRA amplifiers are used [4]. However, such an optical amplifier also generates amplified spontaneous emission (ASE) noise [5], which will limit system performance to an electrical signal to noise ratio at the photodiode determined by the spontaneous-spontaneous and carrier-spontaneous beat noise. Several transmission experiments using distributed Raman amplification technology have been reported, but so far, there are neither theoretical nor experimental reports on the noise performance comparison between the pumping configurations of the low-power pumped Raman amplification system for the middle-distance networks. Thus, based on proposed architecture, we analyze the effects of ASE noise on the performance of DWDM networks using low-power pumped DRA

In this paper, we use theoretical and simulation model of distributed Raman optical amplifier in SMF-28 optical fiber with two different pumping (forward and backward) configurations at pump wavelength of 1470 nm and pump power of 880mW, which is smaller than traditional Raman amplifier's pump. We calculated ASE noise powers and its affection to bit error rate and noise figure of the system. Moreover, we also compare these noise powers with experiment results on the real WDM network system.

II. THEORETICAL ANALYSIS

In this section, we analyze distributed Raman amplification in DWDM transmission systems using both forward and backward pumping. Consider the simplest situation in which a single continuous wave (CW) pump beam is launched into a single-mode fiber with distance L of a transmission system to amplify several CW signals. The evolution of the input signal power of i^{th} channel in DWDM system P_{si} and the input pump power P_p propagating along the single-mode optical fiber in milli-watt, can be expressed by propagation equations that include pump-to-pump, signal-to-signal and pump-to-signal Raman interactions, spontaneous Raman emission and its temperature dependency, stimulated Raman scattering, pump depletions due to Raman energy transfer, high-order Stokes generation, multiple Rayleigh backscattering, fiber loss and spontaneous emission noise, which are the followings [6–10]:

$$\frac{dP_p^\pm}{dz} = \mp \alpha_p P_p^\pm \pm \gamma P_p^\mp \mp \sum_{i=1}^N \frac{f_p}{f_{si}} g_R P_p^\pm P_{si}^\pm \mp \left(\sum_{i=1}^N g_R P_p^\pm h f_{si} \Delta f \right) \left[1 + \frac{1}{e^{h(f_p - f_{si})/k_B T} - 1} \right], \quad (1)$$

$$\frac{dP_{si}^\pm}{dz} = -\alpha_{si} P_{si}^\pm + \gamma P_{si}^\mp + g_R P_p^\pm P_{si}^\pm + 2h f_{si} \Delta f g_R P_p^\pm \left[1 + \frac{1}{e^{h(f_p - f_{si})/k_B T} - 1} \right], \quad (2)$$

$$\frac{dP_n^\pm}{dz} = \mp \alpha_n P_n^\pm \pm \gamma P_n^\mp \pm g_R P_p^\pm P_n^\pm \pm g_R P_p^\pm h f_n \Delta f \left[1 + \frac{1}{e^{h(f_p - f_n)/k_B T} - 1} \right], \quad (3)$$

where g_R is the Raman gain efficiency in $W^{-1}km^{-1}$ of the fiber normalized with respect to the effective area $A_{eff} = \pi r^2$ of the fiber, α_p , α_{si} and α_n are the attenuation coefficients in km^{-1} at the pump, the i^{th} WDM component of the signal and noise frequencies (f_p , f_{si} , and f_n), γ is the Rayleigh backscattering coefficient in km^{-1} . The upper signs of \pm and \mp in three equations correspond to the forward propagating pump and the lower signs correspond to the backward propagating pump. K is the polarization factor ($g_R = g_r / K A_{eff}$), Δf is the frequency interval,

h is Plank's constant, k_B is the Boltzmann's constant and T is the absolute temperature. Noise propagates in both directions with powers P_n^+ and P_n^- .

Two first terms in these equations are fiber loss and Rayleigh backscattering, two last terms in Eq. (1) refer to the signal and the ASE noise induced pump depletion. The third and fourth terms in Eq. (2) include stimulated and spontaneous Raman amplification. The last term in Eq. (3) refers to the spontaneous emission noise power generated at the frequency f_n over a bandwidth Δf . It is possible to derive an explicit analytical solution using a simple iteration method [6] in two following pumping configurations.

II.1. Forward pumping

In forward pumping case, signal and pump waves are propagated from $z = 0$ to $z = L$ in $+z$ direction. By analytical method, the solutions without pump depletion at point z are given as [9]

$$P_p^+(z) = P_p(0) \exp(-\alpha_p z), \quad (4)$$

$$P_{si}(z) = P_{si}(0) \exp \left[-\alpha_{si} z + g_R P_p(0) \frac{1 - \exp(-\alpha_p z)}{\alpha_p} \right], \quad (5)$$

$$\begin{aligned} P_n^+(z) = & \left[h f_n \Delta f \exp(-q_n^+) (q_n^+)^{\alpha_n / \alpha_p} \right. \\ & \times (\Gamma_1(1 + \frac{\alpha_n}{\alpha_p}, q_n^+) - \Gamma_1(1 + \frac{\alpha_n}{\alpha_p}, q_n^+ \exp(-\alpha_s z))) \\ & \left. \times \exp(-\alpha_n z + q_n^+ (1 - \exp(-\alpha_p z))) \right], \end{aligned} \quad (6)$$

$$\begin{aligned} P_n^-(z) = & \left[h f_n \Delta f \exp(q_n^+) (q_n^+)^{-\alpha_n / \alpha_p} \right. \\ & \times (\Gamma_2(1 + \frac{\alpha_n}{\alpha_p}, q_n^+ \exp(-\alpha_s z)) - \Gamma_2(1 + \frac{\alpha_n}{\alpha_p}, q_n^+ \exp(-\alpha_s L))) \\ & \left. \times \exp(-\alpha_n z - q_n^+ (1 - \exp(-\alpha_p z))) \right], \end{aligned} \quad (7)$$

where

$$q_n^+ = \frac{g_R P_p(0)}{\alpha_p}, \quad (8)$$

$$\Gamma_1(\alpha, u) = \int_0^u t^{-\alpha+1} \exp(t) dt, \quad (9)$$

$$\Gamma_2(\alpha, u) = \int_0^u t^{\alpha-1} \exp(-t) dt. \quad (10)$$

II.2. Backward pumping

The backward pumping case can be considered in a similar fashion. Here pump wave is propagated from $z = L$ to 0 in $-z$ direction, solutions of Equations (1), (2), and (3) with pump depletion at point z are given as [9]

$$P_p^-(z) = P_p(L) \exp(-\alpha_p (L - z)), \quad (11)$$

$$P_{si}(z) = P_{si}(0) \exp \left[-\alpha_{si} z + g_R P_p(L) \exp(-\alpha_p L) \frac{\exp(-\alpha_p z) - 1}{\alpha_p} \right] \quad (12)$$

$$P_n^+(z) = \left[hf_n \Delta f \exp(q_n^-) (q_n^-)^{-\alpha_n/\alpha_p} \right. \\ \times \left(\Gamma_2 \left(1 + \frac{\alpha_n}{\alpha_p}, q_n^- \exp(\alpha_s z) \right) - \Gamma_2 \left(1 + \frac{\alpha_n}{\alpha_p}, q_n^- \right) \right) \\ \left. \times \exp(-\alpha_n z + q_n^- (\exp(\alpha_p z) - 1)) \right], \quad (13)$$

$$P_n^-(z) = [hf_n \Delta f \exp(-q_n^-) (q_n^-)^{\alpha_n/\alpha_p} \times \left(\Gamma_1 \left(1 + \frac{\alpha_n}{\alpha_p}, q_n^- \exp(\alpha_s L) \right) \right. \\ \left. - \Gamma_1 \left(1 + \frac{\alpha_n}{\alpha_p}, q_n^- \exp(\alpha_s z) \right) \right) \\ \times \exp(\alpha_n z - q_n^- (\exp(-\alpha_p z) - 1)], \quad (14)$$

where

$$q_n^- = \frac{g_R P_p(L) \exp(-\alpha_p L)}{\alpha_p}. \quad (15)$$

The total variance of the noise intensity is the sum of all variances of thermal noise, shot noise, beat noise and can be written as [11]:

$$\sigma_{total}^2 = \sigma_{th}^2 + \sigma_{shot}^2 + \sigma_{beat}^2. \quad (16)$$

First, the variance of the thermal noise can be written as [2]:

$$\sigma_{th}^2 = \frac{4k_B T B}{R_L}, \quad (17)$$

where, k_B is Boltzmann's constant, T is the receiver temperature, B is the electrical filter bandwidth, and R_L is the load resistance.

Next, the variance of the shot noise, which is generated by signals, and ASE, is given by [11]:

$$\sigma_{shot}^2 = 2qBI_{si} + 2qBI_{ASE}, \quad (18)$$

where

$$I_{si} = P_{si} \frac{q}{hf_{si}}, \quad (19)$$

$$I_{ASE} = 2n_{sp}(G-1)qB, \quad (20)$$

where q is electron charge, G is the average gain of optical amplifier and n_{sp} is population-inversion factor defined as $n_{sp} = n_2/(n_2 - n_1)$.

The last one is beat noise current. It consists of the signals-ASE beat noise, the ASE-ASE beat noise (beating between the spectral components of the added amplifier ASE), and the signal-signal beat noise. The variance of the beat noise is given by [11, 12]:

$$\sigma_{beat}^2 = 2GI_{si}I_{ASE}^{\frac{B}{B_{opt}}} + \frac{1}{2}(I_{ASE})^2 \frac{B(2B_{opt} - B)}{B_{opt}^2} + \frac{1}{2}(GI_{si})^2 \frac{B(2B_{opt} - B)}{B_{opt}^2} \quad (21)$$

where B_{opt} is the optical bandwidth.

Fig. 1 shows the root mean square noise current as a function of the input signal power for bit rate of 10 Gbps, 16 channels, channel space of 0.4 nm and optical amplifier gain of 11 dB. The noise terms contributing significantly to σ_{total}^2 are drawn separately. The beating of the signal-signal and the signal-ASE clearly dominate all other noise terms. It can be said that ASE noise has significantly impact on performance of the DWDM system.

Finally, the bit error rate (*BER*) can be calculated as [2]:

$$BER = \frac{1}{2}erfc(SNR), \tag{22}$$

where $erfc(.)$ is the complementary error function and signal- to- noise rate is written as:

$$SNR = \frac{I_{si}(i^{th})}{\sigma_{total}\sqrt{2}} \tag{23}$$

with $I_{si}(i^{th})$ is photocurrent of i^{th} channel at the output of photodiode.

III. SIMULATION AND EXPERIMENT RESULTS

III.1. Simulation Setup

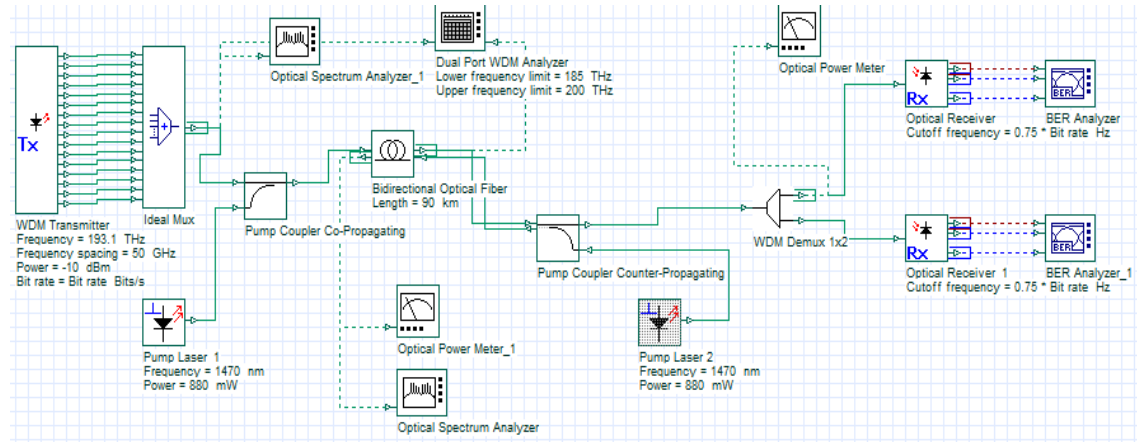


Fig. 2. Block diagram of a DWDM system using distributed Raman amplifier

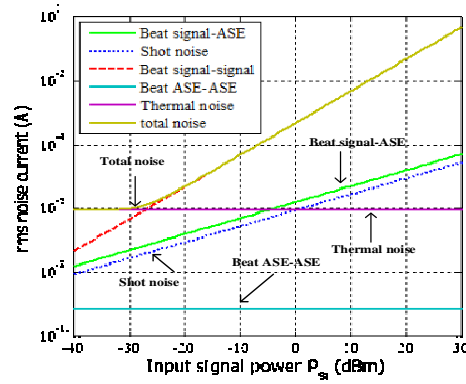


Fig. 1. Noise current versus input signal power at $R_b = 10$ Gbps, $G = 11$ dB and channel space = 0.4 nm

In this section, we set up a DWDM network model by using OptiSystem 7 software to compare ASE noise powers with previous experiment results [13]. In this model, we used a distributed Raman amplifier with different pump configurations, which are forward and backward pumping directions. Fig. 2 shows the system with the propagation of 16 DWDM channels located between 193.1 THz and 193.85 THz, 50 GHz spaced to each other, and a pump wavelength of 1470 nm. A PRBS generator generates the downstream traffic of each channel, which generate pseudo random bit sequences. These bit sequences are then used to control NRZ generators to generate non-return-to-zero signals. On-off-key (OOK) modulation between a NRZ signal and a continuous wave (CW) laser source is carried out by using a Mach-Zehnder modulator. Signals are multiplexed at a multiplexer and then they are combined with the pump at a WDM coupler that transmits them into the bi-directional single-mode optical fiber in the same direction, it is called forward pumping scheme. In the other hand, when a pump laser is located at the output of optical fiber, it is called counter or backward pumping. The signal then will be amplified by stimulated Raman scattering effect in single-mode fiber medium. In the receiver side, the signal is converted into photocurrent by using a PIN photodetector. BER of the received signal is analyzed by using a BER analyzer in combination with a low pass Bessel filter.

III.2. Simulation results

Simulations have been carried out to estimate the effects of ASE noise, noise figure, and chromatic dispersion on performance of network in different pump configurations. Key parameters used for this simulation are listed in Table 1.

Table 1. Simulation parameters

Name	Symbol	Value
Length of DRA	L	0 ÷ 90 km
Effective area	A_{eff}	80 μm^2
Bit rate	R_b	10Gbps
Signal frequency	f_s	193.1 ÷ 193.85 THz
Pump wavelength	λ_p	1470 nm
Pump power	P_p	880 mW
Chromatic dispersion	D	14, 15, 16 ps/ nm.km
Absorption coefficients	α	0.2 dB/km

Fig. 3 shows forward and backward noise powers as a function of the amplifier length of the first signal channel (193.1 THz) when $P_{si} = -10$ dBm and $P_p = 880$ mW. This noises induced by spontaneous Raman scattering as are described in Eqs. (6), (7), (13), and (14). We can see that in the forward pumping case, both forward and backward DRA noise powers are smaller than those in backward pumping. Forward pumping is more advantageous than backward pumping from the viewpoint of minimizing noise.

Fig. 4 shows the noise figure (NF) as a function of the DRA amplifier length for forward and backward pumping. The NF is the ratio of the OSNR at the input of an amplifier to the OSNR at the output of an amplifier. It is a measure of how much the amplifier degrades the signal. As we can see when amplifier length is short, the noise figures of both pumping configurations are the same, but for longer fiber length the different from noise figures becomes remarkable from

the accumulation of noise along the fiber. In addition, the noise figure is not changed when the length of amplifier increases in forward pumping configuration, but this one increases quickly in the backward pumping. This because ASE noise and Double Rayleigh backscattering (DRBS) are larger than those in backward pumping case.

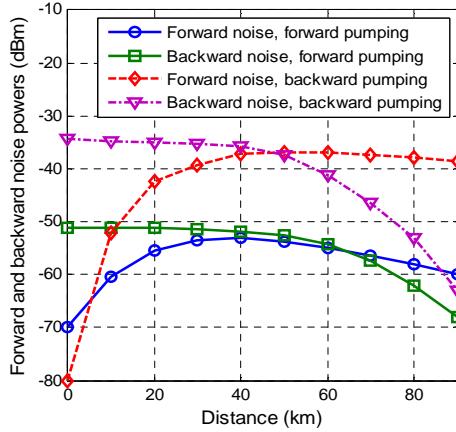


Fig. 3. Noise powers as a function of amplifier length (L) with $P_{si}(0) = -10$ dbm, $P_p = 880$ mW

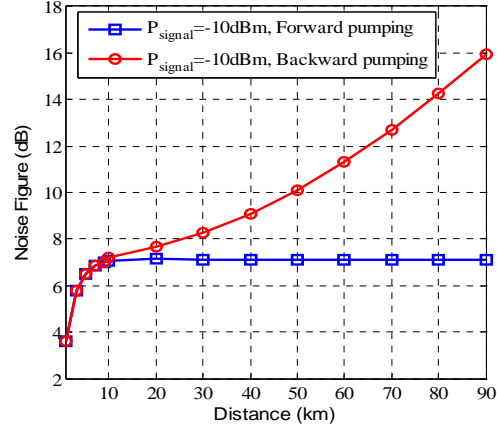


Fig. 4. Noise figure as a function of DRA amplifier length (L) with $P_{si}(0) = -10$ dbm, $P_p = 880$ mW

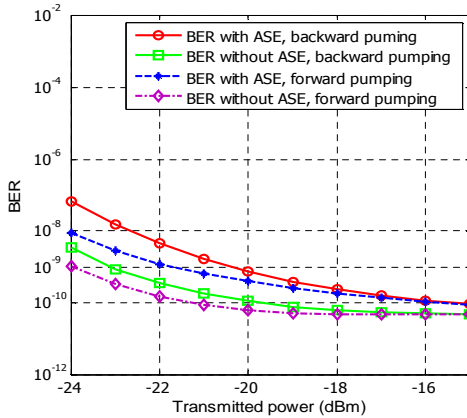


Fig. 5. BER vs. transmitted power with $R_b = 10$ Gbps, $D = 16$ ps/nm.km, $L = 90$ km

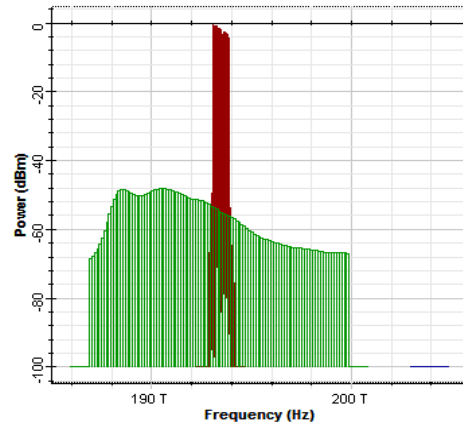


Fig. 6. Amplified signals and ASE noise spectrum, backward pumping

In Fig. 5, we fix chromatic dispersion coefficient $D = 16$ ps/nm.km and the amplifier length of 90 km and investigate BER versus input signal power with and without ASE noise in forward and backward pumping configurations. It is seen that the influence of ASE on the BER increases in backward pumping case. In detail, the power penalty due to ASE noise at BER 10^{-9} is about 2dB for forward pumping, while this one is about 2.3 dB in backward pumping. This result is

consistent with the calculation result from Eqs. (6), (7), (13), and (14), where the ASE noise powers in backward pumping are greater than these in forward pumping.

Fig. 6 shows signals and noise spectrum after being amplified for the backward pumping configuration, which used three pump sources through an optical power combiner, the total pump power is of 880mW. In this case, we fix input signal power $P_{si} = -10\text{dBm}$ and the achieved gain value of the first channel (193.1THz or 1552.52nm) is of 11dB, and noise power in the same channel is about -55dBm . This will decrease the signal-noise-ratio (SNR) of the amplified signal. We will use this result to compare with the experiment result.

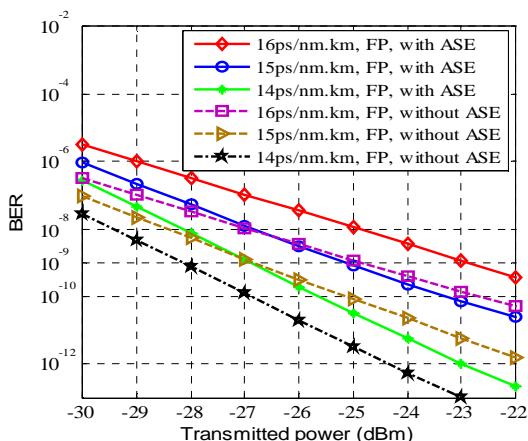


Fig. 7. BER vs. transmitted power with $D = (14, 15, 16)$ ps/nm.km, $L = 90$ km, forward pumping (FP)

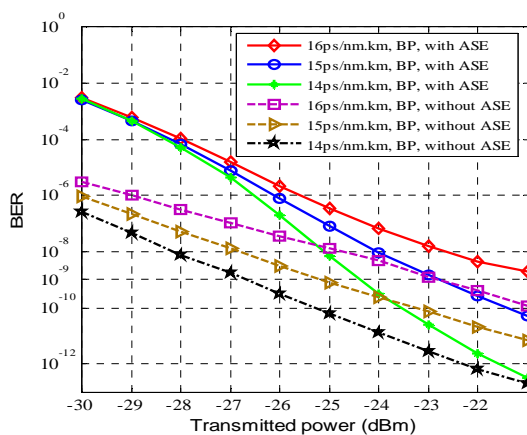


Fig. 8. BER vs. transmitted power with $D = (14, 15, 16)$ ps/nm.km, $L = 90$ km, backward pumping (BP)

Figures 7 and 8 show the dependence of BER on the input signal power for forward and backward pumping with three different values of chromatic dispersion coefficient D of 14, 15, and 16 ps/nm.km. It is seen that, BER increases when D increases. In addition, in forward pumping configuration the power penalties at BER 10^{-9} with and without ASE are smaller than one in backward pumping case. This is consistent with results in Fig. 3 when ASE noise is considered.

III.3. Experiment Results

Experiments have been carried out on the DWDM network, which is operated at 10 GB/s. For no extra-high power pump source is available, we used three low power pump lasers emitted a light at a wavelength of 1470 nm. The total pump power is of 880 mW obtained through an optical power combiner. In this system, we used 1480/1550 WDM coupler for coupling pump power into the fiber where signals pass through it [14].

Fig. 9 shows the results obtained from experiment and simulation for optical signal-noise-ratio (OSNR) in backward pumping case as measured at the output of the optical Raman amplifier. As we can see, when no pump signal is injected into the fiber the OSNR is maximized. Then the OSNR reduces exponentially in both cases for pump power < 200 mW. This is because the pump power over this range is weak and not capable to compensate for losses in the signal, as it propagates through the fiber. The signal power decreases while the pump power is very low will

resulted in decreasing OSNR. When pump power is greater than 200 mW the OSNR gradually increased in both the experiment and the simulation case. However, at pump power above 800mW in the experiment case the OSNR tended to degrade, this is because double Rayleigh scattering is more evident at higher pump powers especially in the backward pumping. This effect has not examined in the simulation scenario, thus two cases are not the same.

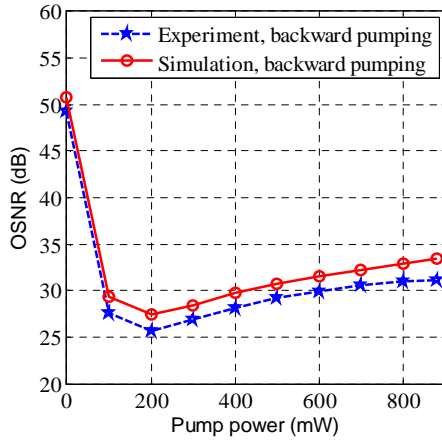


Fig. 9. OSNR as a function of pump power, backward pumping

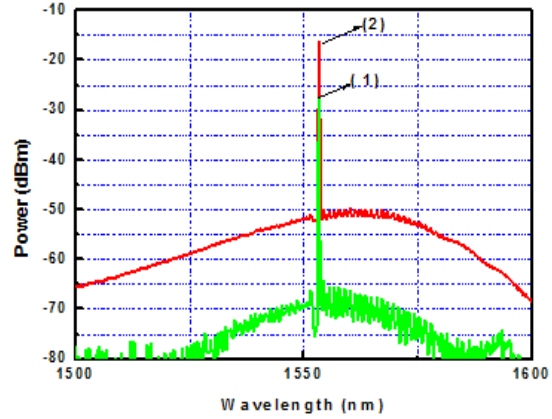


Fig. 10. Signal without (curve 1) and with optical gain (curve 2) for $L=90\text{km}$ and $P_p=880\text{ mW}$

Fig. 10 shows signal spectrum at a wavelength of 1552.52nm and related signal power in the case of Raman amplification in comparison with non-amplification. It is seen that the signal amplified up to 11dB while its bandwidth and wavelength are no change. However, the OSNR of amplified signal is of 31dB, which is decreased on 6dB in comparison with non-amplified one (37dB). This result shows that the total noise σ_{total}^2 is increased about 15dB by the ASE-beat noise, when the thermal and shot noise are the same in an experimental condition. The calculation result of noise current and SNR by formulas (16, 23) are depicted on the Fig. 1 and the above simulation results very well agree with this experiment result. Moreover, we find that the ASE noise power of the experiment is 2dB greater than one of the simulation that because we do not examine the affection of double Rayleigh scattering and nonlinear effects.

IV. CONCLUSION

We have analyzed the theory and simulated a DWDM network system using a low-power pumped distributed Raman amplifier in two different pump directions. Moreover, we analyzed the effects of ASE noise, noise figure, and chromatic dispersion on the performance of DWDM-based system. We found that the different pumping configurations and ASE noise play an important role in network performance. Simulation results show that the low bit error rate and noise figure were obtained when using forward pumping configuration for the fiber amplifier length of 90 km. The calculation results are also compared with the experimental one, and they are well matched. In addition, the amplification of DRA depends on both power and wavelength pump. From this

study, we conclude that distributed Raman amplifier with low power pump ($P_{pump} < 1$ W is low power in comparison with this one more than 1.5 W) is the promising key technology for short- and/or middle-distance DWDM transmission networks.

ACKNOWLEDGMENTS

This work has been supported in part by the 2015 Project of University of Engineering and Technology. The authors would like to thank the Center of High Tech Communication, Department of Telecom for their support of experiments on DWDM network.

REFERENCES

- [1] J. M. Senior, *Optical Fiber Communications: Principles and Practice*, Publisher S. K. Kataria & Sons, New Delhi, 2005.
- [2] C. Headley and G. Agrawal, *Raman amplification in fiber optical communication systems*, Elsevier Academic Press, 2005.
- [3] M. Wasfi, *International Journal of Communication Networks and Information Security (IJCNIS)* **1** (1) (2009) 42–47.
- [4] S. Singh, M. Sharma, and R. Kaur, *International Journal of Advanced Computer Science and Applications (IJACSA), Special Issue on Wireless & Mobile Networks* (2011) 76–80.
- [5] R. Róka and F. Čertík, *International Journal of Communication Networks and Information Security (IJCNIS)* **4** (3) (2012) 144–162.
- [6] L. Zhang, S. Wang, and C. Fan, *Optics Communications* **197** (4) (2001) 459–465.
- [7] D. Dahan and G. Eisenstein, *Journal of Lightwave Technology* **20** (3) (2002) 379–388.
- [8] I. Mandelbaum and M. Bolshtyansky, *Photonics Technology Letters, IEEE* **15** (12) (2003) 1704–1706.
- [9] D. Dahan and G. Eisenstein, *Optics Communications* **236** (4) (2004) 279–288.
- [10] M. A. P. de Andrade, J. Anacleto, and J. M. M. de Almeida, *Simulation of Various Configurations of Single-pump Dispersion-compensating raman/EDFA Hybrid Amplifiers*, Integrated Optoelectronic Devices 2007, International Society for Optics and Photonics, 2007, p. 646807.
- [11] G. Keiser, *Optical fiber communications*, Fourth edition, McGraw-Hill, 2011.
- [12] M. Jazayerifar, S. Warm, R. Elschner, D. Kroushkov, I. Sackey, C. Meuer, C. Schubert, and K. Petermann, *Journal of Lightwave Technology* **31** (9) (2013) 1454–1461.
- [13] W. Mathlouthi, M. Menif, and L. A. Rusch, *Beat Noise Effects on Spectrum-sliced WDM*, Applications of Photonic Technology, International Society for Optics and Photonics, 2003, pp. 44–54.
- [14] N. T. Bui, T. Q. Nguyen, and H. V. Pham, *International Journal of Communication Networks and Information Security (IJCNIS)* **6** (2) (2014) 168–172.